


ORIGINAL ARTICLE

Metformin normalizes the structural changes in glycogen preceding prediabetes in mice overexpressing neuropeptide Y in noradrenergic neurons

Liisa Ailanen^{1,2} | Natalia N. Bezborodkina³ | Laura Virtanen¹ | Suvi T. Ruohonen¹ | Anastasia V. Malova³ | Sergey V. Okovityi⁴ | Elizaveta Y. Chistyakova⁴ | Eriika Savontaus^{1,5} 

¹Institute of Biomedicine, Research Center for Integrative Physiology and Pharmacology and Turku Center for Disease Modelling, University of Turku, Turku, Finland

²Drug Research Doctoral Program, University of Turku, Turku, Finland

³Laboratory of Cellular Pathology, Institute of Cytology of the Russian Academy of Sciences, St. Petersburg, Russia

⁴Department of Pharmacology and Clinical Pharmacology, Saint-Petersburg State Chemical Pharmaceutical Academy, St. Petersburg, Russia

⁵Unit of Clinical Pharmacology, Turku University Hospital, Turku, Finland

Correspondence

Eriika Savontaus, University of Turku, Institute of Biomedicine, Kiinamyllynkatu 10, 20520 Turku, Finland.
Email: eriika.savontaus@utu.fi

Abstract

Hepatic insulin resistance and increased gluconeogenesis are known therapeutic targets of metformin, but the role of hepatic glycogen in the pathogenesis of diabetes is less clear. Mouse model of neuropeptide Y (NPY) overexpression in noradrenergic neurons (OE-NPY^{DβH}) with a phenotype of late onset obesity, hepatosteatosis, and prediabetes was used to study early changes in glycogen structure and metabolism preceding prediabetes. Furthermore, the effect of the anti-hyperglycemic agent, metformin (300 mg/kg/day/4 weeks in drinking water), was assessed on changes in glycogen metabolism, body weight, fat mass, and glucose tolerance. Glycogen structure was characterized by cytofluorometric analysis in isolated hepatocytes and mRNA expression of key enzymes by qPCR. OE-NPY^{DβH} mice displayed decreased labile glycogen fraction relative to stabile fraction (the intermediate form of glycogen) suggesting enhanced glycogen cycling. This was supported by decreased filling of glucose residues in the 10th outer tier of the glycogen molecule, which suggests accelerated glycogen phosphorylation. Metformin reduced fat mass gain in both genotypes, but glucose tolerance was improved mostly in wild-type mice. However, metformin inhibited glycogen accumulation and normalized the ratio between glycogen structures in OE-NPY^{DβH} mice indicating decreased glycogen synthesis. Furthermore, the presence of glucose residues in the 11th tier together with decreased glycogen phosphorylase expression suggested inhibition of glycogen degradation. In conclusion, structural changes in glycogen of OE-NPY^{DβH} mice point to increased glycogen metabolism, which may predispose them to prediabetes. Metformin treatment normalizes these changes and suppresses both glycogen synthesis and phosphorylation, which may contribute to its preventive effect on the onset of diabetes.

Abbreviations: IGT, impaired glucose tolerance; IR, insulin resistance; LF, labile glycogen fraction; NPY, neuropeptide Y; SF, stabile glycogen fraction; T2D, type 2 diabetes; TCA, trichloroacetic acid; TGC, total glycogen content; WT, wild type.

This is an open access article under the terms of the Creative Commons Attribution-NonCommercial-NoDerivs License, which permits use and distribution in any medium, provided the original work is properly cited, the use is non-commercial and no modifications or adaptations are made.

© 2018 The Authors. *Pharmacology Research & Perspectives* published by John Wiley & Sons Ltd, British Pharmacological Society and American Society for Pharmacology and Experimental Therapeutics.

KEYWORDS

glycogen structure, metformin, neuropeptide Y, prediabetes

1 | INTRODUCTION

Type 2 diabetes (T2D) is a complex disorder of glucose metabolism characterized by insulin resistance (IR), that leads to compensatory hyperinsulinemia and increased hepatic glucose output resulting in decreased glucose uptake in insulin-sensitive tissues (liver, skeletal muscle, and adipose tissue) and increased hepatic glucose production. Glucose is stored in tissues as glycogen, but liver is the only organ capable of producing glucose from glycogen (reviewed by Kowalski et al¹). The role of hepatic glycogen in the pathogenesis of diabetes is controversial and unclear in many aspects.²⁻⁵ However, increased glycogenolysis and glycogen cycling have been associated with diabetes in both rodents and humans.^{6,7} Fitting with this, it has been suggested that glycogen degrades more rapidly in T2D, which could explain the uncontrolled hepatic glucose output.⁸

The liver glycogen is stored in the form of individual molecules (full-size glycogen molecules, β -particles), which construct larger α -particle conglomerates consisting of 20-40 β -particles.⁹⁻¹¹ Individual glycogen molecules are composed of 2 fractions with different solubility in trichloroacetic acid (TCA): a highly soluble labile glycogen fraction (LF; lyoglycogen), which forms the 4 outer tiers of glycogen particles, and a less metabolically active form, stabile glycogen fraction (SF; desmoglycogen).¹² It has been under debate whether the labile glycogen corresponds to larger glycogen particles (with molecular mass of $\sim 10^7$ Da) and the stabile glycogen to smaller protein (glycogenin)-binding particles (with mass of $\sim 4 \times 10^5$ Da), and about their actual physiological meanings.¹³⁻¹⁶ However, there is an agreement on the existence of glycogen particles with different solubility in TCA, and that changes occur in the ratio of the labile and stabile structures (LF/SF ratio) in different physiological and pathological conditions.¹⁷ In a physiological glycogen synthesis, when fasted animals are administered with glucose, the stabile fraction is initially quickly increased, but then the labile fraction increases being responsible for the actual glycogen accumulation.¹⁸ In contrast, in a pathologic situation of liver cirrhosis, the stabile fraction is especially increased and the ratio of LF/SF decreased, suggesting a more stable increase in glycogen.¹⁹⁻²² It can be hypothesized that similar molecular changes in glycogen structure could also occur in diabetes, as similar disruptions in glycogen metabolism have been shown to occur in cirrhosis and diabetes,²³ and α -particles of glycogen have been shown to degrade more readily in diabetes.⁸ However, it is not known whether the structural changes contribute to the disease pathogenesis, and whether these changes could be targeted by drug therapy.

The aim of this study was to characterize the hepatic glycogen structure and metabolism in a state preceding disruptions in glucose metabolism, and after metformin therapy. The state preceding

impaired glucose tolerance (IGT) was modeled by a transgenic mouse overexpressing neuropeptide Y (NPY) in noradrenergic neurons (OE-NPY^{D^{BH}}). These mice are known to develop prediabetes with obesity, IR and IGT with age, and show increased susceptibility to T2D induced by high caloric diet and low-dose streptozotocin.²⁴⁻²⁶ Hepatic accumulation of triglycerides and glycogen seem to play an important role in the development of prediabetes and streptozotocin-induced diabetes in the model.²⁴ Our previous findings suggest that increased glycogen cycling precedes glycogen accumulation, but it is not known, whether the changes are detected also in the glycogen structure. Furthermore, we chose metformin as the reference drug, because the main mechanism of its anti-hyperglycemic effect is to decrease hepatic glucose production, and as it has been shown to attenuate the progression of prediabetes to diabetes.²⁷⁻²⁹

2 | MATERIALS AND METHODS

2.1 | Animals

Homozygous male OE-NPY^{D^{BH}} mice (n = 9-11/group) were used in this study with their wild-type (WT) controls. Generation of the transgenic homozygous OE-NPY^{D^{BH}} mice, maintained on a C57BL/6N inbred background, and their metabolic phenotype have been described in detail previously.^{24,26} The age of the mice in the current experiment was 4 months at the initiation of metformin treatment, which is the borderline age when the first signs of IR (ie, increased glucose-stimulated insulinemia and IGT) start to emerge eventually leading to clear prediabetic phenotype at the age of 7 months.

2.2 | Study protocol

The study was authorized by the Finnish National Animal Experiment Board (ELLA). Animal care was in accordance with the guidelines of the International Council of Laboratory Animal Science (ICLAS). Mice were kept in an animal room maintained at $21 \pm 3^\circ\text{C}$ with a fixed 12-hour light/dark cycle. A standard rodent chow (SDS, Essex, UK) and tap water were available ad libitum. Mice were housed in individual cages starting from age of 8 weeks. Food intake and body weights were measured once a week throughout the study starting at age of 14 weeks. At 16 weeks, body composition was measured in vivo with quantitative NMR (EchoMRI-700; Echo Medical Systems, Houston, TX, USA) in order to divide OE-NPY^{D^{BH}} and WT mice into 2 treatment groups matched for weight, fat mass, and food intake. At 17 weeks, mice received drinking water either with or without metformin (300 mg/kg/day; Enzo Life Sciences LTD, Exeter, UK) for 4 weeks. The water bottles were changed and weighed twice a week. The consumption was calculated by subtracting the

final bottle weight from the starting weight and then subtracting the estimated leakage. The value for leakage was based on testing the average leakage of bottles in cages without mice. The water consumption was around 1 mL/10 g body weight, and there were no differences between the treatments and genotypes. Thus, the average daily metformin dose was as planned and similar between the genotypes (WT 300.3 ± 11.8 mg/kg/day, OE-NPY^{D β H} 283.1 ± 10.7 mg/kg/day, $P = .30$). The body composition measurement was repeated prior to the start of drug administration and at sacrifice (at age of 21 weeks). Glucose tolerance test (1 g/kg glucose intraperitoneally) was performed at age of 20 weeks, as described previously.²⁶ At sacrifice, 4 hour-fasted mice were sedated with CO₂, and serum was obtained by cardiac puncture. Liver was perfused and hepatocytes were isolated from 5 mice per group as described below, or dissected and weighed. Samples were stored in -70°C .

2.3 | Hepatocyte isolation and structure analysis

Hepatocyte isolation was performed according to Kudryavtseva et al.³⁰ Mouse liver ($n = 3\text{-}7/\text{group}$) was perfused for 10 minutes in a K,Na-phosphate-sucrose buffer I, pH = 7.8 (475 mL Na₂HPO₄ \times 2H₂O, 25 mL KH₂PO₄, 500 mL sucrose). A piece of liver was placed into buffer I for 20 min, and further a $2 \times 2 \times 2$ mm piece was incubated in a phosphate buffer II, pH = 7.2 (400 mL Na₂HPO₄ \times 2H₂O, 100 mL KH₂PO₄) for 5 minutes. Smears of isolated hepatocytes were prepared by gentle shaking of the pieces in a drop of buffer II using tweezers. The cell suspension obtained was spread over the surface of a slide using quartz glass with a polished edge and fixed with methanol.

The preparations of smears of isolated hepatocytes ($n = 3\text{-}7/\text{group}$) were stained with a fluorescent variant of the periodic acid-Schiff (PAS) reaction for identification of glycogen fractions in isolated hepatocytes. The presence of 2 glycogen fractions in the cells stained in situ with the use of cytochemical techniques corresponds to different solubility of the fractions in TCA.^{18,30-32} Preparations were placed into sodium periodate solution in diluted HNO₃ (200 mg of sodium periodate, 25 mL of 0.23% HNO₃) for 1.5 hours. The oxidized preparations were washed under running tap water for 5 minutes and once in distilled water. To detect the labile fraction, the preparations were placed in EtBr-SO₂ (100 mL 10⁻⁵ mol/L ethidium bromide, 0.2 mL thionyl chloride) for 40 min, rinsed in distilled water, and finally placed in Au-SO₂ (300 mg auramine, 100 mL water, 0.2 mL thionyl chloride) for 50 minutes to detect the stabile fraction of glycogen. After the staining, preparations were washed in distilled water and in sulfurous water (5 g potassium metabisulfite, 950 mL of water, 50 mL of HCl) 3 times for 3 minutes each. Finally, preparations were washed under running tap water for 20 min, rinsed in distilled water, and dehydrated in alcohols of increasing concentrations (70, 96, and 100 vol.% for 5 minutes in each change of alcohols).

Images of the Au-SO₂ and EtBr-SO₂ stained cells (Figure 1) were obtained using an Axioskop microscope (Carl Zeiss, Oberkochen, Germany), a Plan NEOFLUAR 40 \times 0.75 lens, and a DFC360 FX

digital high-sensitivity CCD camera (1392 \times 1400). To excite, Au-SO₂ and EtBr-SO₂ fluorescence interference filters at 450-490 and 546 nm were used, and to record fluorescence interference filters at 515-565 and 590 nm were used, respectively. The intensity of fluorescence of the cells stained with Au-SO₂ and EtBr-SO₂ was measured using ImageJ software (National Institute of Health, USA). The total glycogen content (TGC) in each cell was taken to be equal to the sum of glycogen fractions. The fluorescence of 100 cells was measured for each preparation. The relative number of glucose residues in the outer tiers of the glycogen molecule was calculated using the data on the number of glucose chains that were calculated according to the theoretical formulations of the Whelan's model.³³ As labile fraction constitutes the first 8 tiers of the glycogen molecule and consists of 255 glucose chains, it has been accepted that the LF/SF ratio that is ≤ 1 corresponds to the ninth tier, the LF/SF ratio that is ≤ 2 corresponds to the 10th tier, LF/SF ratio that is ≤ 4 corresponds to the 11th tier, and LF/SF ratio that is ≤ 8 corresponds to the 12th end tier of the molecule.

2.4 | Gene expression analyses

Samples for RNA isolation ($n = 9\text{-}11/\text{group}$) were stored in RNA Stabilization Reagent (RNAlater, Qiagen, Hilden, Germany). Liver RNA was extracted with Trizol Reagent (Invitrogen, Carlsbad, CA, USA) with DNase treatment (Sigma-Aldrich, St. Louis, MO, USA). RNA was converted to cDNA with High Capacity RNA-to-cDNA Kit (Applied Biosystems, Foster City, CA, USA). mRNA expression was analyzed with SYBR Green (KAPA SYBR[®] FAST ABI Prism[®]; Kapa Biosystems, Woburn, MA) technique using 7300 Real-Time PCR System (Applied Biosystems). The expression of target genes was quantified relative to geometrical mean of reference genes (β -actin and ribosomal protein S29). Primers used for quantification are shown in Table 1.

2.5 | Statistical analysis

Statistical processing of glycogen contents were analyzed with Student's *t* test, using SigmaPlot v 11.0 software (Systat Software Inc., San Jose, CA). All the other parameters were analyzed with GraphPad Prism 6.0 software (GraphPad Software, Inc., San Diego, CA). Tests with multiple time points were analyzed with repeated measures two-way ANOVA. Parameters with single time points were analyzed with two-way ANOVA taking into account the genotype and drug effects, and their interaction, and were followed by Bonferroni post hoc tests when interaction was significant. The results are expressed as means \pm SEM. $P < .05$ was considered statistically significant.

3 | RESULTS

3.1 | Body composition and food intake

OE-NPY^{D β H} mice in this study, in contrast to previous reports, were similar in body weight and adiposity compared to WT mice

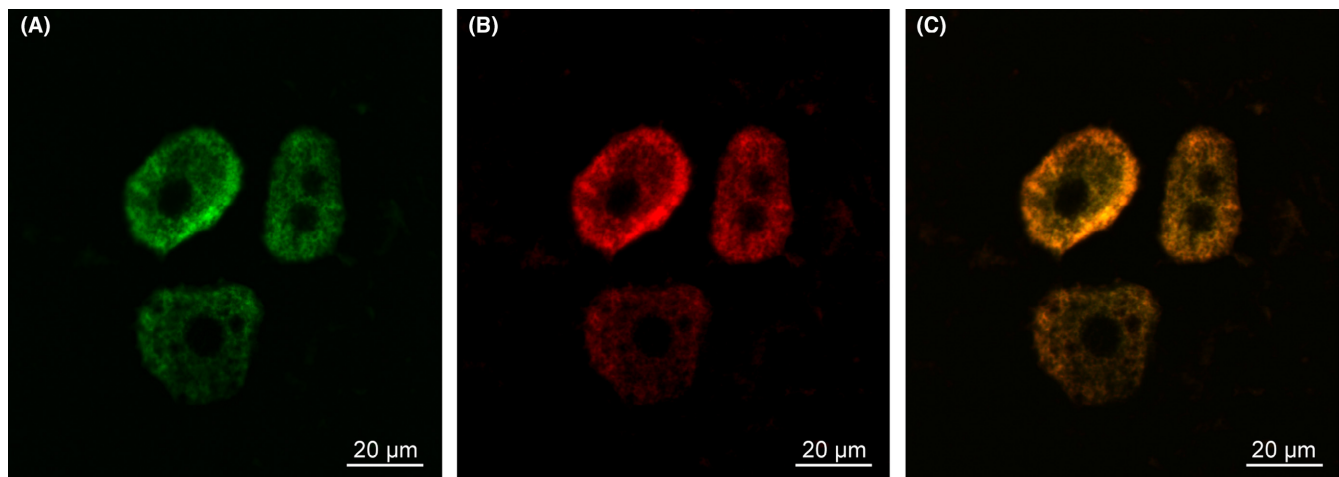


FIGURE 1 Images of glycogen structures in hepatocytes. (A) Stable fraction was stained with Au-SO₂ and (B) labile fraction with EtBr-SO₂. (C) Total glycogen content is the combination of these 2 structures

TABLE 1 qPCR primers

Gene name	Forward 5'-3'	Reverse 5'-3'
<i>Bact</i> , beta actin	tccatcatgaagtgtgacgt	gagcaatgatcttgatcttcat
<i>Gys2</i> , glycogen synthase 2	cgatgctgtcagaaaagctg	agccatcttccaaaatgcac
<i>G6p</i> , glucose-6-phosphatase	cgactcgctatctccaagtga	ggcgcttgcacaacagaat
<i>Pck1</i> , phosphoenolpyruvate carboxykinase 1, cytosolic	agcattcaacgccaggttc	cgagtctgtagttcaatacca
<i>Ppargc1a</i> , peroxisome proliferative activated receptor, gamma, coactivator 1 alpha	tatggagtgcacatagagtgtgct	ccacttcaatcccaccagaaag
<i>Pygl</i> , liver glycogen phosphorylase	ccagagtgtctaccccaat	ccaccacaagtagtctctgtttc
<i>S29</i> , Ribosomal protein S29	atgggtcaccagcagctcta	agcctatgtccttcgcgtact

(Figure 2A and B). To note, WT mice were mildly obese for their age, likely due to single housing. Metformin significantly decreased gain in body weight and whole body fat mass over the treatment period in both genotypes (Figure 2C and D). The decrease in adiposity was mainly due to a decrease in visceral fat and was more pronounced in WT mice, as retroperitoneal fat tended to be smaller in metformin-treated groups ($P = .075$), but mesenteric adipose tissue depot was significantly smaller in metformin-treated WT mice compared to controls, but not in OE-NPY^{DβH} mice (Figure 2E). Metformin did not influence the sizes of other WAT depots (epididymal, inguinal subcutaneous) (Figure 2E), interscapular brown fat or the liver in either genotype (data not shown). There were no significant differences in absolute (Figure 2F) or cumulative food intake between treatment groups (Metformin-treated WT 107.2 ± 1.2 g/day and OE-NPY^{DβH} 109.2 ± 1.8 g/day vs control WT 111.8 ± 1.5 g/day and OE-NPY^{DβH} 111.6 ± 2.9 g/day; Treatment effect $P = .08$).

3.2 | Glucose metabolism

Fasting blood glucose was similar between treatment groups and genotypes (Figure 3A). GTT revealed no difference between genotypes in glucose clearance fitting with similar body weights and

adiposity between genotypes. Metformin treatment reduced the increase in glucose (area under the curve, AUC) during the first 20-min period being more pronounced in WT mice without affecting the clearance rate of glucose at 20-90-min period (Figure 3B-D). The more pronounced therapeutic effect in WT mice could be due to decreased adiposity as AUC values of GTT positively correlated with fat mass ($r = .655$, $P < .05$), but not lean mass. There were no differences in the mRNA expressions of known targets of metformin: the gluconeogenic enzymes phosphoenolpyruvate carboxykinase 1 (*Pck1*), glucose-6-phosphatase (*G6pc*), or peroxisome proliferator-activated receptor gamma coactivator 1-alpha (*Pgc1a*) (Figure 3E-G).

3.3 | Glycogen molecule structure in OE-NPY^{DβH} mice

In order to detect glycogen structure preceding prediabetes, TGC and the glycogen fractions were analyzed from OE-NPY^{DβH} and WT mice receiving drinking water without metformin. TGC in hepatocytes was similar between the genotypes. However, OE-NPY^{DβH} mice showed a decreased content of the labile fraction and an increased content of the stable fraction resulting in reduced LF/SF ratio, which suggests enhancement of glycogen synthesis (Table 2). TGC correlated significantly with both the labile ($r = .933$, $P < .001$)

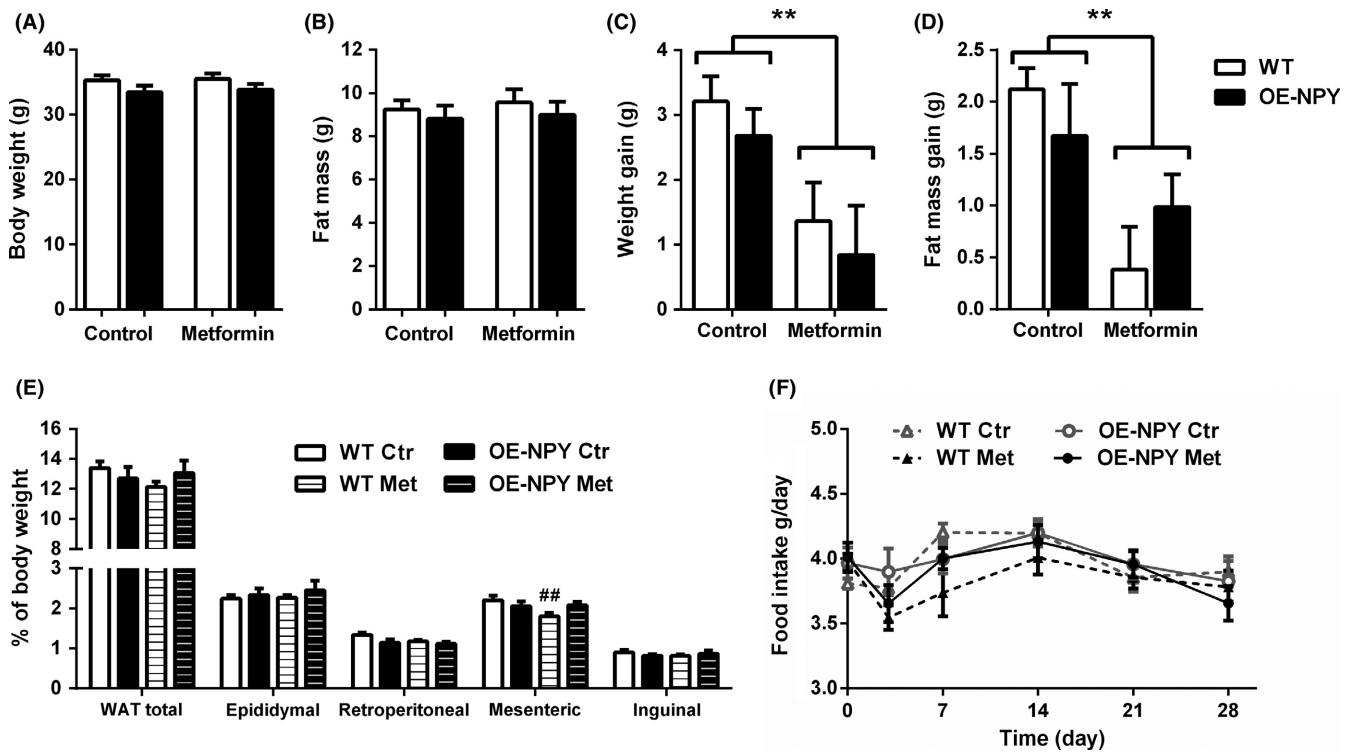


FIGURE 2 The effect of metformin on the phenotype of OE-NPY^{DβH} vs WT mice. (A) Baseline body weight, (B) baseline fat mass, (C) weight gain, (D) fat mass gain, (D) sizes of different fat pads, and (E) daily food intake of OE-NPY^{DβH} vs WT mice (n = 9-11/group) receiving drinking water with (Met) or without (Ctr) metformin for 4 weeks. Values are expressed as means ± SEM. **P < .01 between the treatments with two-way ANOVA (C-D). ##P < .01 Bonferroni post hoc comparison between metformin-treated and control WT mice, two-way ANOVA indicated a tendency to treatment x genotype interaction (P = .08)

and the stable fraction content ($r = .896, P < .001$) in WT hepatocytes. In OE-NPY^{DβH} mice, correlation between the parameters was similar, but less pronounced ($r = .696, P < .001$ and $r = .712, P < .001$, respectively).

The filling of the tiers of the glycogen molecule was analyzed according to Whelan's model. The 10th tier of the glycogen in WT mice was filled, on average, by 81.7% indicating constant regulation of blood glucose. Instead in OE-NPY^{DβH} mice, the 10th tier was only filled by 58.4%, suggesting enhanced activity of glycogen phosphorylase (Table 3).

3.4 | Effects of metformin on glycogen structure

In order to study whether metformin influences the glycogen content or structure, TGC and different glycogen fractions were analyzed from OE-NPY^{DβH} and WT mice receiving metformin for 4 weeks, and compared to control groups. There was no change in glycogen content or structure in WT mice between the treatments. However, metformin treatment markedly decreased the content of the stabile fraction and significantly also the content of the labile fraction in OE-NPY^{DβH} resulting in reduced TGC and normalization of the LF/SF ratio to the level of the WT group (Table 1). Furthermore, the composition of glycogen residues to the 11th tier of glycogen molecule was present in metformin-treated OE-NPY^{DβH} mice pointing to a decreased glycogen phosphorylase activity as glycogen phosphorylase is responsible for

degradation of upper tiers of glycogen molecules (Table 2). In accordance, mRNA expression of glycogen phosphorylase (*Pygl*) was significantly decreased in metformin-treated OE-NPY^{DβH} mice. No differences were detected in WT mice, between genotypes in control-treated mice, or in glycogen synthase (*Gys*) expression between the treatment groups (Figure 4A-B).

4 | DISCUSSION

Metformin is the first-line anti-diabetic agent to treat T2D, but multiple studies have shown that metformin is also effective in preventing or delaying the onset of T2D.²⁷⁻²⁹ Metformin improves insulin sensitivity by decreasing hepatic glucose production due to decreased ATP availability,^{6,34} but also several other contributing mechanisms have been reported.³⁵⁻³⁷ The roles of gluconeogenesis as a source of hepatic glucose overproduction and as a target of metformin action are well described, but less is known about the role of changes in glycogen structure and metabolism, especially in prediabetic state. In this study, we show that early phase changes in glycogen structure may contribute to the development of IGT and diabetes, and treatment with metformin in this early phase decreases hepatic glycogen levels and normalizes glycogen structure, which may have therapeutic relevance in prevention of the onset of prediabetes or diabetes.

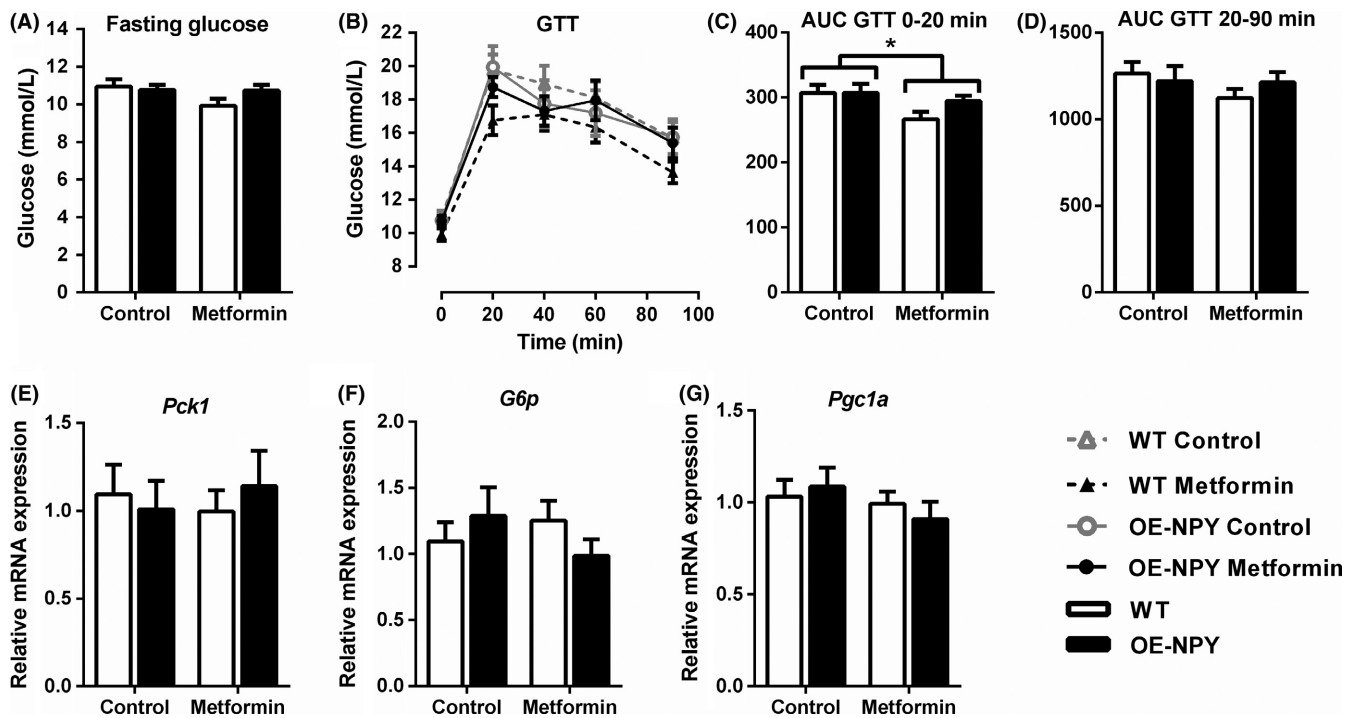


FIGURE 3 Glucose metabolism in metformin-treated OE-NPY^{DβH} vs WT mice. (A) Fasting (4 hours) blood glucose, (B) glucose tolerance test, and (C) AUC of glucose tolerance test at 0-20 minutes and (D) 20-90 minutes periods of OE-NPY^{DβH} vs WT mice (n = 9-11/group) after 3 weeks of receiving drinking water with or without metformin. (E-F) mRNA expression of gluconeogenic enzymes in the livers of OE-NPY^{DβH} vs WT mice (n = 9-11/group) after 4 weeks of receiving drinking water with or without metformin. Values are expressed as means ± SEM. **P < .05 between the treatments with two-way ANOVA. AUC, area under curve; GTT, glucose tolerance test; *Pck1*, phosphoenolpyruvate carboxylase 1; *G6pc*, glucose-6-phosphatase; *Pgc1a*, peroxisome proliferative activated receptor, gamma, coactivator 1 alpha

TABLE 2 The contents of different glycogen structures (standard units) in hepatocytes of metformin-treated OE-NPY^{DβH} vs WT mice

Genotype	Treatment	SF	LF	TGC	LF/SF
WT	Ctr	10.59 ± 0.39	17.63 ± 0.58	28.53 ± 0.97	1.63 ± 0.02
	Met	9.25 ± 0.39	15.38 ± 0.63	25.41 ± 1.04	1.51 ± 0.04
OE-NPY	Ctr	14.25 ± 0.49**	12.90 ± 0.42**	30.87 ± 0.98	0.62 ± 0.02***
	Met	5.49 ± 0.21***, ###	10.65 ± 0.44***, #	16.48 ± 0.65***, ###	1.70 ± 0.04###

The data are represented as mean ± SEM (n = 3 mice/group). SF, stable fraction; LF, labile fraction; TGC, total glycogen content; Met, metformin-treated group.

P < .01 and *P < .001 compared to WT mice receiving drinking water without metformin (Ctr), and #P < .05, ###P < .001 compared to OE-NPY^{DβH} mice receiving drinking water without metformin (Ctr) with Student's t test.

TABLE 3 The filling of outer tiers of glycogen molecules with respect to the content of glucose residues (%) in hepatocytes of metformin-treated OE-NPY^{DβH} vs WT mice

Genotype	Treatment	Outer tiers		
		9th	10th	11th
WT	Ctr	100	81.7	—
	Met	100	83.7	—
OE-NPY	Ctr	100	58.4	—
	Met	100	100	52.5

The calculations were performed from 100 hepatocytes with Whelan's model. Ctr, control group receiving drinking water without metformin; Met, metformin-treated group; WT, wild-type.

The glycogen structure was elucidated in a genetically modified mouse model of prediabetes, OE-NPY^{DβH} mouse, at an age prior to manifestation of overt IGT in order to evaluate our previous findings of increased hepatic glycogen cycling (ie, increased mRNA expression of glycogen synthase and phosphorylase) preceding glycogen accumulation.²⁴ Despite equal glycogen contents and similar glucose tolerance between the genotypes, changes in the molecular structure of glycogen in OE-NPY^{DβH} hepatocytes, that is, increased content of the stable fraction and decreased content of the labile fraction supported by decreased filling of the 10th tier in the glycogen molecules, suggest that increased glycogen synthesis and degradation takes place before prediabetes. Using the same cytofluorometric analysis similar changes in glycogen structure were detected in

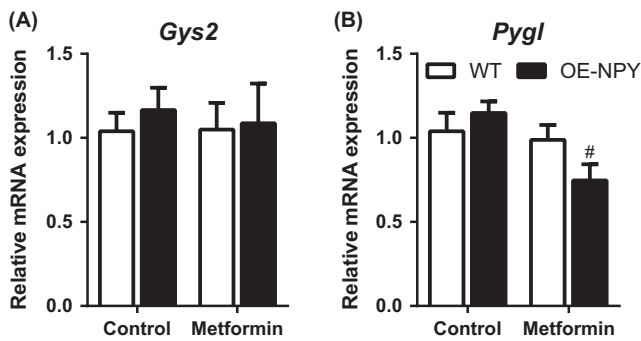


FIGURE 4 mRNA expression of glycogen synthase and phosphorylase in metformin-treated OE-NPY^{DBH} vs WT mice. (A) mRNA expression of glycogen synthase and (B) phosphorylase enzymes in the livers of OE-NPY^{DBH} vs WT mice (n = 9-11/group) after 4 weeks of receiving drinking water with or without metformin. Values are expressed as means ± SEM. [#]P < .05 Bonferroni post hoc comparison between metformin-treated and control OE-NPY^{DBH} mice, two-way ANOVA indicated a tendency to treatment × genotype interaction (P = .06). *Gys2*, glycogen synthase 2; *Pygl*, liver glycogen phosphorylase

another chronic pathologic condition, liver cirrhosis.^{18,19} This is opposite to the situation of physiological glycogen synthesis, (eg, in glucose administration after a prolonged fast), where the metabolically active form, labile glycogen, is rapidly increased.^{18,38} Previous data on glycogen structure and metabolism in prediabetes is scarce, but increased glycogen metabolism has also been reported in prediabetic Zucker (fa/fa) rats.³⁹ In T2D, glycogen metabolism has received more attention, showing increased glycogen metabolism^{6,7,40} and fragility of the α -particles of glycogen.^{3,8,40} However, as the glycogen content in diabetes varies between the studies^{5,41-43} depending on the type (1 or 2) and the state (early or established) of diabetes, and the diurnal cycle,^{7,40,44} accelerated glycogen metabolism and the structure of glycogen molecules seem to be better biomarkers for pathogenic glucose metabolism than the glycogen content itself.

We next studied the effect of metformin on hepatic glycogen structure. In OE-NPY^{DBH} hepatocytes, metformin decreased the contents of total and both structural forms of glycogen. Furthermore, supported by decreased *Pygl* mRNA expression, increased LF/SF ratio and filling of the 11th tier in the glycogen molecule indicate that glycogen phosphorylase activity was inhibited. When glycogen phosphorylase does not decompose glycogen fast enough and there is no formation of new molecules, glycogen synthase and the branching enzyme attach glucose residues to glycogen molecules that are already formed. As the overall glycogen content was decreased, it seems that also glycogen synthesis was decreased by metformin. Our results reinforce the previous finding of metformin's ability to reduce glycogen degradation.⁴⁵⁻⁴⁷ However, we show that this is the case already in an early phase, before the actual symptoms of IGT. Therefore, this could be a mechanism of action in decreasing hepatic glucose output especially in a situation of prediabetic enhancement of glycogen accumulation and cycling. Inhibition of glycogen phosphorylase activity is known to improve glucose metabolism and has previously been

studied as a potential drug target for treating hyperglycemia.⁴⁸⁻⁵⁰ Furthermore, metformin's ability to inhibit glycogen synthesis has previously been suggested by others,⁵¹⁻⁵³ although opposite findings also occur.⁴⁷ Similar to diabetes, the results on metformin-induced changes in total hepatic glycogen content have been more controversial and depended on the model used (ie, severity of the disease and in vivo or in vitro study).^{46,47,51}

Although potentially beneficial changes in glycogen metabolism were detected in metformin-treated OE-NPY^{DBH} mice, glucose tolerance was not markedly improved, which is not unexpected in glucose-tolerant mice.⁵⁴ Instead, metformin-treated WT mice displayed mild improvement in glucose tolerance, possibly due to decreased visceral adiposity, as no response in glycogen structure was detected. Nevertheless, it remains open whether the progression of IGT in OE-NPY^{DBH} mice would have been prevented due to the changes in glycogen structure (ie, normalization of LF/SF ratio), had we continued the follow-up longer or started the treatment with metformin in established IGT.

In conclusion, this study shows that the overall glycogen metabolism and the content of stable fraction are increased in a prediabetic OE-NPY^{DBH} model even preceding IGT and glycogen accumulation, and may thus contribute to the progression of the disease, or to NPY-induced metabolic disruptions. Metformin significantly changes the structure of glycogen especially by diminishing the content of uncomplete stable fraction, and suppresses both glycogen synthesis and phosphorylation. This may contribute to its anti-hyperglycemic effect in diseased condition, or to its inhibiting effects on progression of the disease potentially providing novel targets for drug development in treating prediabetes or T2D.

ACKNOWLEDGEMENTS

The authors thank Salla Juhantalo, Sanna Bastman, and Satu Mäkelä (Institute of Biomedicine, University of Turku, Turku, Finland) for technical assistance.

DISCLOSURES

The authors do not declare any conflict of interest.

ORCID

Eriika Savontaus  <http://orcid.org/0000-0003-3421-0367>

REFERENCES

1. Kowalski GM, Bruce CR. The regulation of glucose metabolism: implications and considerations for the assessment of glucose homeostasis in rodents. *Am J Physiol Endocrinol Metab.* 2014;307:E859-E871.
2. Macauley M, Smith FE, Thelwall PE, Hollingsworth KG, Taylor R. Diurnal variation in skeletal muscle and liver glycogen in humans with normal health and Type 2 diabetes. *Clin Sci.* 2015;128:707-713.

3. Roesler WJ, Pugazhenth S, Khandelwal RL. Hepatic glycogen metabolism in the db/db mouse. *Mol Cell Biochem.* 1990;92:99-106.
4. Sogujko Y, Krivko Y, Krikun E. Ultrastructural characteristics of rats liver in norm and in experimental diabetes mellitus on late terms of run. *Med Pharm.* 2013;21:147-150.
5. Tomiyasu M, Obata T, Nishi Y, et al. Monitoring of liver glycogen synthesis in diabetic patients using carbon-13 MR spectroscopy. *Eur J Radiol.* 2010;73:300-304.
6. Hundal RS, Krssak M, Dufour S, et al. Mechanism by which metformin reduces glucose production in type 2 diabetes. *Diabetes.* 2000;49:2063-2069.
7. Roesler WJ, Khandelwal RL. Age-related changes in hepatic glycogen metabolism in the genetically diabetic (db/db) mouse. *Diabetes.* 1985;34:395-402.
8. Deng B, Sullivan MA, Li J, et al. Molecular structure of glycogen in diabetic liver. *Glycoconj J.* 2015;32:113-118.
9. Devos P, Baudhuin P, Van Hoof F, Hers HG. The alpha particulate liver glycogen. A morphometric approach to the kinetics of its synthesis and degradation. *Biochem J.* 1983;209:159-165.
10. Rybicka KK. Glycosomes—the organelles of glycogen metabolism. *Tissue Cell.* 1996;28:253-265.
11. Sullivan MA, Vilaplana F, Cave RA, Stapleton D, Gray-Weale AA, Gilbert RG. Nature of alpha and beta particles in glycogen using molecular size distributions. *Biomacromol.* 2010;11:1094-1100.
12. Calder PC. Glycogen structure and biogenesis. *Int J Biochem.* 1991;23:1335-1352.
13. James AP, Barnes PD, Palmer TN, Fournier PA. Proglycogen and macroglycogen: artifacts of glycogen extraction? *Metabolism.* 2008;57:535-543.
14. Katz A. Glycogenin, proglycogen, and glycogen biogenesis: what's the story? *Am J Physiol Endocrinol Metab.* 2006;290:E757-E758; author reply E758-9.
15. Lomako J, Lomako WM, Whelan WJ. Proglycogen: a low-molecular-weight form of muscle glycogen. *FEBS Lett.* 1991;279:223-228.
16. Shearer J, Graham TE. New perspectives on the storage and organization of muscle glycogen. *Can J Appl Physiol.* 2002;27:179-203.
17. Barnes PD, Singh A, Fournier PA. Homogenization-dependent responses of acid-soluble and acid-insoluble glycogen to exercise and refeeding in human muscles. *Metabolism.* 2009;58:1832-1839.
18. Bezborodkina NN, Shtein GI, Sivova EV, Chestnova AY, Kudryavtsev BN. Analysis of structure of glycogen in rat hepatocytes using cytochemical and FRET methods. *Cell Tissue Biol.* 2011;5:417.
19. Kudryavtseva MV, Emelyanov AV, Sakuta GA, Bezborodkina NN, Kudryavtsev BN. Glycogen-forming function of hepatocytes in the rat regenerating cirrhotic liver after a partial hepatectomy. *Tissue Cell.* 1998;30:261-267.
20. Kudryavtseva M, Bezborodkina NN, Okovity SV, Kudryavtsev BN. Metabolic heterogeneity of glycogen in hepatocytes of patients with liver cirrhosis: the glycogen of the liver lobule zones in cirrhosis. *Eur J Gastro Hepatol.* 2001;13:693-697.
21. Kudryavtseva MV, Bezborodkina NN, Okovity SV, Kudryavtsev BN. Effects of the 2-ethylthiobenzimidazole hydrobromide (bemithyl) on carbohydrate metabolism in cirrhotic rat liver. *Exp Toxicol Pathol.* 2003;54:339-347.
22. Kudryavtseva MV, Sakuta GA, Skorina AD, Stein GI, Emelyanov AV, Kudryavtsev BN. Quantitative analysis of glycogen content in hepatocytes of portal and central lobule zones of normal human liver and in patients with chronic hepatitis of different etiology. *Tissue Cell.* 1996;28:279-285.
23. Wu C, Okar DA, Kang J, Lange AJ. Reduction of hepatic glucose production as a therapeutic target in the treatment of diabetes. *Curr Drug Targets Immune Endocr Metabol Disord.* 2005;5:51-59.
24. Ailanen L, Ruohonen ST, Vahatalo LH, et al. The metabolic syndrome in mice overexpressing neuropeptide Y in noradrenergic neurons. *J Endocrinol.* 2017;234:57-72.
25. Ruohonen ST, Pesonen U, Moritz N, et al. Transgenic mice overexpressing neuropeptide Y in noradrenergic neurons: a novel model of increased adiposity and impaired glucose tolerance. *Diabetes.* 2008;57:1517-1525.
26. Vahatalo LH, Ruohonen ST, Makela S, et al. Neuropeptide Y in the noradrenergic neurones induces obesity and inhibits sympathetic tone in mice. *Acta Physiol.* 2015;213:902-919.
27. Knowler WC, Barrett-Connor E, Fowler SE, et al. Reduction in the incidence of type 2 diabetes with lifestyle intervention or metformin. *N Engl J Med.* 2002;346:393-403.
28. Li CL, Pan CY, Lu JM, et al. Effect of metformin on patients with impaired glucose tolerance. *Diabet Med.* 1999;16:477-481.
29. Ramachandran A, Snehalatha C, Mary S, et al. The Indian Diabetes Prevention Programme shows that lifestyle modification and metformin prevent type 2 diabetes in Asian Indian subjects with impaired glucose tolerance (IDPP-1). *Diabetologia.* 2006;49:289-297.
30. Kudryavtseva MV, Besborodkina NN, Kudryavtsev BN. Restoration of the glycogen-forming function of hepatocytes in rats with liver cirrhosis is facilitated by a high-carbohydrate diet. *Br J Nutr.* 1999;81:473-480.
31. Kudryavtseva MV, Kudryavtsev BN, Rozanov YM. Two glycogen fractions in rat liver cells (cytofluorometric study). *Tsitologiya.* 1974;16:851-858.
32. Kugler JH, Wilkinson WJ. The basis for the histochemical detection of glycogen. *J Histochem Cytochem.* 1961;9:498-503.
33. Roach PJ. Glycogen and its metabolism. *Curr Mol Med.* 2002;2:101-120.
34. Madiraju AK, Erion DM, Rahimi Y, et al. Metformin suppresses gluconeogenesis by inhibiting mitochondrial glycerophosphate dehydrogenase. *Nature.* 2014;510:542-546.
35. Mannucci E, Tesi F, Bardini G, et al. Effects of metformin on glucagon-like peptide-1 levels in obese patients with and without Type 2 diabetes. *Diabetes Nutr Metab.* 2004;17:336-342.
36. Wu T, Thazhath SS, Bound MJ, Jones KL, Horowitz M, Rayner CK. Mechanism of increase in plasma intact GLP-1 by metformin in type 2 diabetes: stimulation of GLP-1 secretion or reduction in plasma DPP-4 activity? *Diabetes Res Clin Pract.* 2014;106:e3-e6.
37. Yasuda N, Inoue T, Nagakura T, et al. Enhanced secretion of glucagon-like peptide 1 by biguanide compounds. *Biochem Biophys Res Comm.* 2002;298:779-784.
38. Kudryavtseva MV, Stein GI, Shashkov BV, Kudryavtsev BN. Functional activity of human hepatocytes under traumatic disease. *Exp Toxicol Pathol.* 1998;50:53-57.
39. Jin ES, Park BH, Sherry AD, Malloy CR. Role of excess glycogenolysis in fasting hyperglycemia among pre-diabetic and diabetic Zucker (fa/fa) rats. *Diabetes.* 2007;56:777-785.
40. Sullivan MA, Harcourt BE, Xu P, Forbes JM, Gilbert RG. Impairment of liver glycogen storage in the db/db animal model of type 2 diabetes: a potential target for future therapeutics? *Curr Drug Targets.* 2015;16:1088-1093.
41. Krssak M, Brehm A, Bernroider E, et al. Alterations in postprandial hepatic glycogen metabolism in type 2 diabetes. *Diabetes.* 2004;53:3048-3056.
42. Magnusson I, Rothman DL, Katz LD, Shulman RG, Shulman GI. Increased rate of gluconeogenesis in type II diabetes mellitus. A 13C nuclear magnetic resonance study. *J Clin Invest.* 1992;90:1323-1327.
43. Whitton PD, Hems DA. Glycogen synthesis in the perfused liver of streptozotocin-diabetic rats. *Biochem J.* 1975;150:153-165.
44. Roesler WJ, Helgason C, Gulka M, Khandelwal RL. Aberrations in the diurnal rhythms of plasma glucose, plasma insulin, liver glycogen, and hepatic glycogen synthase and phosphorylase activities in genetically diabetic (db/db) mice. *Horm Metab Res.* 1985;17:572-575.
45. Chu CA, Wiernsperger N, Muscato N, Knauf M, Neal DW, Cherrington AD. The acute effect of metformin on glucose production in the conscious dog is primarily attributable to inhibition of glycogenolysis. *Metabolism.* 2000;49:1619-1626.

46. Wang X, Chen Y, Abdelkader D, Hassan W, Sun H, Liu J. Combination therapy with oleanolic acid and metformin as a synergistic treatment for diabetes. *J Diabetes Res.* 2015;2015:973287.
47. Xu H, Zhou Y, Liu Y, et al. Metformin improves hepatic IRS2/PI3K/Akt signaling in insulin-resistant rats of NASH and cirrhosis. *J Endocrinol.* 2016;229:133-144.
48. Martin WH, Hoover DJ, Armento SJ, et al. Discovery of a human liver glycogen phosphorylase inhibitor that lowers blood glucose in vivo. *Proc Natl Acad Sci USA.* 1998;95:1776-1781.
49. Nagy L, Docsa T, Szanto M, et al. Glycogen phosphorylase inhibitor N-(3,5-dimethyl-Benzoyl)-N'-(beta-D-glucopyranosyl)urea improves glucose tolerance under normoglycemic and diabetic conditions and rearranges hepatic metabolism. *PLoS ONE.* 2013;8:e69420.
50. Ogawa AK, Willoughby CA, Bergeron R, et al. Glucose-lowering in a db/db mouse model by dihydropyridine diacid glycogen phosphorylase inhibitors. *Bioorg Med Chem Lett.* 2003;13:3405-3408.
51. Alengrin F, Grossi G, Canivet B, Dolais-Kitabgi J. Inhibitory effects of metformin on insulin and glucagon action in rat hepatocytes involve post-receptor alterations. *Diabete Metab.* 1987;13:591-597.
52. Heishi M, Ichihara J, Teramoto R, et al. Global gene expression analysis in liver of obese diabetic db/db mice treated with metformin. *Diabetologia.* 2006;49:1647-1655.
53. Otto M, Breinholt J, Westergaard N. Metformin inhibits glycogen synthesis and gluconeogenesis in cultured rat hepatocytes. *Diabetes Obes Metab.* 2003;5:189-194.
54. Tang X, Li J, Xiang W, et al. Metformin increases hepatic leptin receptor and decreases steatosis in mice. *J Endocrinol.* 2016;230:227-237.

How to cite this article: Ailanen L, Bezborodkina NN, Virtanen L, et al. Metformin normalizes the structural changes in glycogen preceding prediabetes in mice overexpressing neuropeptide Y in noradrenergic neurons. *Pharmacol Res Perspect.* 2018;e00389. <https://doi.org/10.1002/prp2.389>